Available online at www.sciencedirect.com
ScienceDirect
Applied Catalysis B: Environmental 82 (2008) 19–26
APPLIED CATALYSIS B: ENVIRONMENTAL
www.elsevier.com/locate/apcatb

MnO_x modified Co_3O_4-CeO_2 catalysts for the preferential oxidation of CO in H_2-rich gases

Qiang Guo, Yuan Liu *

Department of Catalysis Sciences and Technology, School of Chemical Engineering, Tianjin University, Tianjin 300072, PR China

Received 16 October 2007; received in revised form 13 December 2007; accepted 8 January 2008
Available online 18 January 2008

Abstract

In this work, MnO_x modified Co_3O_4-CeO_2 catalysts were prepared and used for preferential oxidation of CO in hydrogen-rich gases. The catalytic performance tests results showed that the catalyst with Co:Ce:Mn molar ratio of 8:1:1 exhibited the best low-temperature CO oxidation activity and higher selectivity for CO-PROX reaction among tested catalysts. 100% CO conversion could be obtained over this catalyst at 80–180 °C with the feeding gas of 1 vol.% CO, 1 vol.% O_2, 50 vol.% H_2 and N_2 balance under the space velocity of $40,000\,ml\,h^{-1}\,g_{cat}^{-1}$. Adding CO_2 and/or water was unfavorable for CO removal, even so complete oxidation of CO was still achieved over this catalyst with the reaction stream of 20 vol.% CO_2, 10 vol.% H_2O, 1 vol.% CO, 1 vol.% O_2, 50 vol.% H_2 and N_2 balance under high space velocity of $80,000\,ml\,h^{-1}\,g_{cat}^{-1}$ at reaction temperature range of 160–180 °C. The catalysts were characterized by XRD, TEM, EDX, TPR and XPS techniques and the results showed that adding MnO_x into Co_3O_4-CeO_2 led to more uniform mixing of Co_3O_4 and CeO_2 particles and led to finely dispersed and high valence state cobalt oxides species, which contributed to high catalytic activity of Co-Ce-Mn mixed oxides catalysts.

Keywords: MnO_x; Co_3O_4; CeO_2; Preferential oxidation; CO; Hydrogen

1. Introduction

Proton exchange membrane fuel cell (PEMFC) is an attractive technology for power generation mainly due to its high efficiency and environmental friendship [1]. Hydrogen as fuel for PEMFC can be produced by steam reforming or autothermal reforming of hydrocarbons in combination with water gas shift (WGS) reaction. The effluent gases from the WGS reaction process typically contain about 40–75 vol.% H_2, 20–25 vol.% CO_2, 10 vol.% H_2O, N_2 (if air is an oxidant), and 0.5–2 vol.% CO [2]. The anodes of fuel cells, however, can easily be poisoned by CO. The content of CO in the streams, as a result, must be reduced to below 10 ppm for Pt anode and below 100 ppm for CO-tolerant alloy anodes before feeding [3]. Several different methods for CO removal have been studied including purification with metal membrane, preferential oxidation (PROX) of CO, and CO methanation. Among all of them, preferential oxidation of CO with oxygen or air is now considered as the simplest and most effective method for removing CO from hydrogen-rich streams [4].

The reported promising catalysts for CO-PROX can be grouped into three types: (1) supported noble metal catalysts, such as Pt, Pd or Rh [5–11], (2) nano-gold catalysts [12–17] and (3) base metal oxides catalysts which mainly concentrate on CuO-CeO_2 [18–22]. Noble metal catalysts and CuO-CeO_2 catalyst are active for CO-PROX in higher reaction temperature range of 150–300 °C. Gold catalysts exhibit high activity for CO oxidation at lower temperature, ca.<100 °C. High activity at low reaction temperature is favorable for improving the cold-start properties in fuel cell system and for compacting the PROX unit and the PEM fuel cell stacks [23]. However, CO removal to below 10 ppm is hard to be achieved over gold catalysts due to their high activities for hydrogen oxidation, although Au catalysts are reported to be very active for CO oxidation at low temperature. Therefore, developing catalysts for CO-PROX with high selectivity as well as good low-temperature activity is of great significance.

CoO_x/CeO_2 catalysts are very active for CO oxidation and their high activities are ascribed to finely dispersed and high

* Corresponding author. Tel.: +86 22 87401675.
E-mail addresses: tjguoqiang@yahoo.com.cn (Q. Guo), yuanliu@tju.edu.cn (Y. Liu).

0926-3373/$ – see front matter © 2008 Elsevier B.V. All rights reserved.
doi:10.1016/j.apcatb.2008.01.007

valence state CoO_x which results from the synergistic interaction between cobalt oxides and ceria [24,25]. At present, little information on CoO_x/CeO_2 for CO-PROX reaction has been published, although a few catalysts containing cobalt, such as $CoFe_2O_4$, Co-Pt/TiO_2, Co/$SrCO_3$, were reported for CO-PROX [26–28].

In our previous work, the catalytic performance of Co_3O_4-CeO_2 catalysts for preferential oxidation of CO in hydrogen-rich gases was examined and it was found that adding a small mount of ceria into Co_3O_4 led to obvious improvement of the catalytic activity for CO-PROX [29].

In this work, it was found that MnO_x modified Co_3O_4-CeO_2 exhibited much better catalytic performance for CO preferential oxidation at low temperature (<80 °C) and exhibited a broad temperature window for complete CO removal.

2. Experimental

2.1. Catalyst preparation

MnO_x modified Co_3O_4-CeO_2 catalysts were prepared by co-precipitation method as described in the previous work [29]. The aqueous solutions of $Ce(NO_3)_3{\cdot}6H_2O$, $Co(NO_3)_2{\cdot}6H_2O$ and $Mn(NO_3)_2{\cdot}6H_2O$ were mixed at desired ratios. Then the mixed solutions and a sodium carbonate solution were gradually and simultaneously dropped into a continuously stirred flask at a pH value of 8.5–9.5. After an aging period of 4 h, the resulting precipitates were filtered and washed with hot water until no pH change, and then they were dried under static air at 80 °C for 24 h and calcined at 350 °C for 5 h. The so prepared catalysts were denoted as *a*Co-*b*Ce-*c*Mn, in which *a*, *b* and *c* represented the molar ratio of Co, Ce and Mn.

2.2. Catalytic performance tests

The catalytic performance tests were carried out with a fixed bed flow reactor system under atmospheric pressure. Catalysts were preoxidized with gas mixture of 5 vol.% O_2/N_2 at 300 °C for 40 min on-line. Then the reactor was cooled to reaction temperature. The reaction gas mixture consisted of 1 vol.% CO, 1 vol.% O_2, 50 vol.% H_2 and N_2 balance. The influence of CO_2 and/or H_2O on the preferential oxidation of CO was examined by adding 20 vol.% CO_2 and/or 10 vol.% H_2O into the feeding gases. The outlet gas mixtures from the reactor were analyzed with a gas chromatograph system equipped with TCD and FID detectors. A nickel catalytic converter was used for detecting trace mount of CO. Thus, CO content below 10 ppm could be detected.

2.3. Catalyst characterization

X-ray diffraction (XRD) measurements were performed by using X'pert Pro diffractometer equipped with a Co Kα X-ray tube operating at 40 kV and 40 mA. The particle size of the samples was calculated by the Sherrer formula.

Transmission electron microscopy (TEM) analysis of catalysts was performed using a Philips G2 F-20 Microscope equipped with energy-dispersive X-ray (EDX) instrument.

Temperature-programmed reduction (TPR) experiments were performed in a micro-flow reactor fed with 5.0% H_2/Ar mixture flowing at a rate of 30 ml/min. The weight of tested samples was 50 mg. Prior to each tests, the samples were treated with N_2 gas at 40 °C for 30 min. Then the temperature was raised from 40 to 930 °C at a heating rate of 10 °C/min. The hydrogen consumption was measured by TCD detector, calibrated by the peak area of known amounts of CuO.

X-ray photoemission spectroscopy (XPS) analysis of catalysts was performed using PERKIN ELMER PHI 1600 spectrometer equipped with a Mg Kα source at a beam power of 250 W. Extended spectra (survey) were collected in the range of 0–1350 eV (187.85 eV pass energy). The binding energy (BE) was calibrated with a reference of taking the C 1s photoelectron peak located at 284.6 eV of ''adventitious'' carbon.

3. Results and discussion

3.1. Catalytic performance

Fig. 1 shows CO conversion and selectivity to CO oxidation for PROX reaction over 8Co-1Ce and Co-Ce-Mn catalysts with different molar ratios. As could be seen from Fig. 1, catalytic activity was improved markedly by adding a small mount of MnO_x to Co–Ce mixed oxides. CO could be completely oxidized to CO_2 over 8Co-1Ce-1Mn catalyst at a low temperature of 80 °C, which was rarely observed over base metal oxides catalysts [18–22,24,25] and was even comparable to noble metal catalysts [6–11].

Besides, 8Co-1Ce-1Mn catalyst exhibited high selectivity for CO oxidation, which was higher than gold catalysts. At the reaction temperature of 80 °C, CO conversion and corresponding selectivity were 100% and 98.2%, respectively, over 8Co-1Ce-1Mn catalyst. Gold-based catalysts were characterized with high low-temperature activity for CO oxidation, while their selectivities for CO-PROX were relatively poor. Chang et al. [13] found 1% Au/$Mn_{0.5}$-$Ce_{0.5}O_2$ exhibited very good catalytic performance for CO-PROX and Grisel et al. [17] also gave an excellent work on Au/MnO_x/MgO/Al_2O_3 for CO-PROX. However, due to poor selectivity caused by H_2 oxidation in CO-PROX process, CO was hard to be removed to below 10 ppm over both of these Au catalysts.

8Co-1Ce-1Mn catalyst exhibited an interesting and attractive character, that is, complete oxidation of CO could be obtained in a broad reaction temperature range from 80 to 180 °C, as presented in Fig. 1a.

The activity of Co-Ce-Mn catalysts for CO oxidation decreased sharply with increasing the molar ratio of MnO_x. Complete CO removal could hardly be obtained over 4Co-1Ce-4Mn. This indicated that MnO_x was not the key active component for CO oxidation.

Fig. 2 presents the influence of space velocity on CO conversion over 8Co-1Ce-1Mn catalyst. As space velocity was doubled, the curve of CO conversion changed a little; as it was trebled, 100% CO conversion could still be achieved between 120 and 180 °C, indicating that this catalyst was very active.

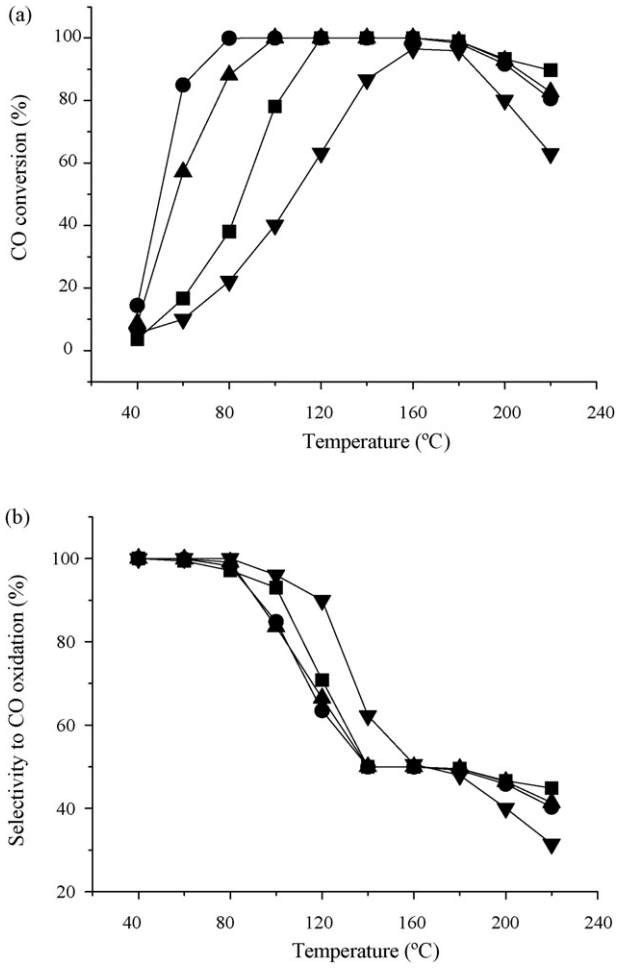

Fig. 1. Variation of CO conversion (a) and selectivity to CO oxidation (b) with reaction temperature over catalysts of (■) 8Co-1Ce, (●) 8Co-1Ce-1Mn, (▲) 6Co-1Ce-2Mn and (▼) 4Co-1Ce-4Mn in the reaction mixture of 1 vol.% CO, 1 vol.% O_2, 50 vol.% H_2 and N_2 balance under space velocity of $40,000\,ml\,h^{-1}\,g_{cat}^{-1}$.

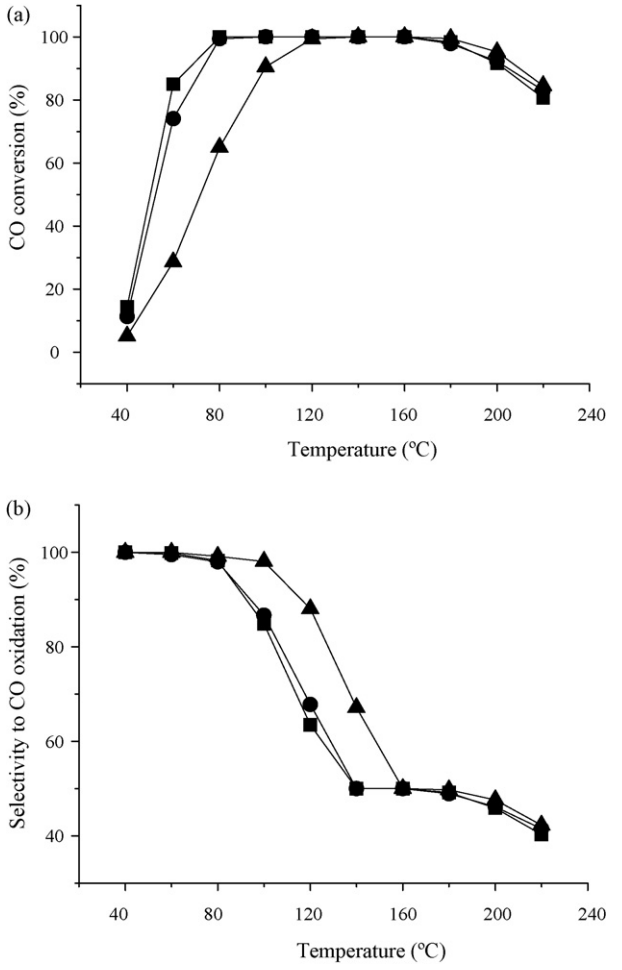

Fig. 2. Variation of CO conversion (a) and selectivity to CO oxidation (b) with reaction temperature over 8Co-1Ce-1Mn catalyst for CO-PROX under space velocities of (■) 40,000, (●) 80,000 and (▲) $120,000\,ml\,h^{-1}\,g_{cat}^{-1}$.

Fig. 3 shows the influence of CO_2 and/or H_2O on CO conversion. CO_2 or H_2O in the feeding streams led to a decrease of CO conversion. Even so, when both CO_2 and H_2O were added into the reaction gases, complete removal of CO could still be obtained at 160–180 °C under a high space velocity of $80,000\,ml\,h^{-1}\,g_{cat}^{-1}$.

The variation of CO conversion with reaction time over 8Co-1Ce-1Mn catalyst is presented in Fig. 4. It could be seen that CO conversion dropped quickly after about 1100 min running. As the catalyst was treated with the gas of N_2 at 300 °C for 30 min, it was partially reactivated. Then treated with gas mixtures of 5% H_2/N_2 at 250 °C and 5% O_2/N_2 at 300 °C for 30 min respectively, the catalyst was fully reactivated.

It was proposed that cobalt oxides for CO oxidation could deactivate by CO_2 via adsorption or formation of carbonate species [24,30]. The adsorbed CO_2 would be partially desorbed by flowing N_2 gas at 300 °C, which led to the catalyst partially reactivated. The adsorbed CO_2 and carbonate species on CoO_x-CeO_2 surface could readily react with hydrogen to produce CO via reverse water gas shift reaction or to form methane via methanation at about 250 °C. Hence, treating with hydrogen could remove the adsorbed CO_2, and the catalyst could be completely reactivated. This meant that the deactivation should be caused by the retention of CO_2 or carbonate species as suggested in literature [24].

3.2. Characterization

Fig. 5 shows the XRD patterns of 8Co-1Ce-1Mn and 8Co-1Ce catalysts. In the XRD patterns, only Co_3O_4 and CeO_2 phases could be observed, meaning that MnO_x existed as highly dispersed or amorphous species. With the addition of manganese oxides into 8Co-1Ce sample, the diffraction peaks of Co_3O_4 and CeO_2 became broader and the average particle size of Co_3O_4 decreased from around 12.9 to 10.5 nm.

The TEM images of 8Co-1Ce catalyst are given in Fig. 6. At high magnification (Fig. 6A), Co_3O_4 particles could be observed by the presence of ordered fringers with a space distance between crystal face of 0.465 nm typical of crystalline Co_3O_4. The particle size of Co_3O_4 was between 10 nm and 15 nm tested by the TEM which was consistent with the calculated results from the XRD measurements.

The EDX results indicated that CeO_2 particles were not dispersed uniformly in 8Co-1Ce catalyst as shown in

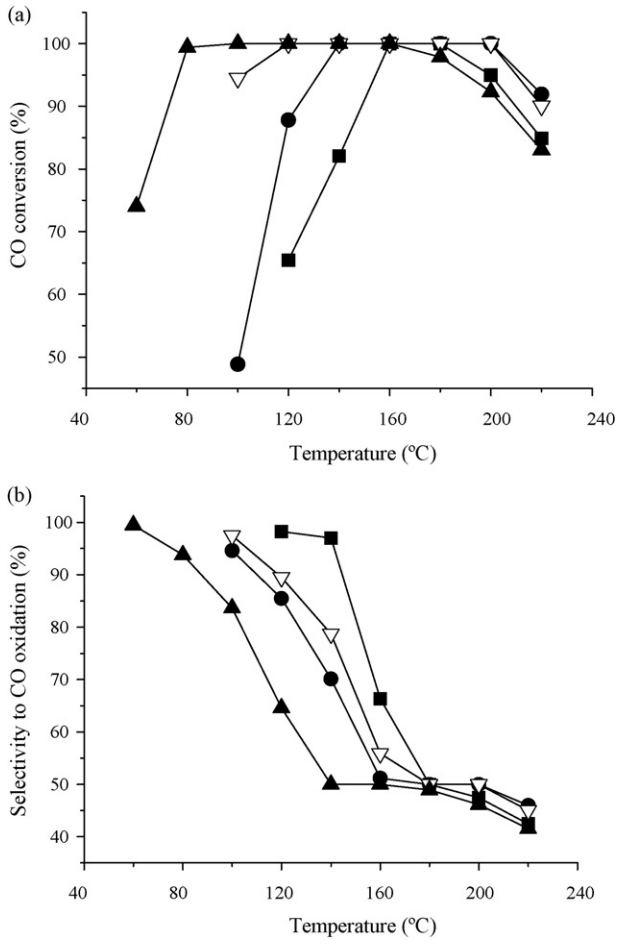

Fig. 3. Variation of CO conversion (a) and selectivity to CO oxidation (b) with reaction temperature over 8Co-1Ce-1Mn catalyst for CO-PROX in reaction mixtures of (■) 1 vol.% CO, 1 vol.% O_2, 50 vol.% H_2, 20 vol.% CO_2, 10 vol.% H_2O and N_2; (●) 1 vol.% CO, 1 vol.% O_2, 50 vol.% H_2, 20 vol.% CO_2 and N_2; (▽) 1 vol.% CO, 1 vol.% O_2, 50 vol.% H_2, 10 vol.% H_2O and N_2; (▲) 1 vol.% CO, 1 vol.% O_2, 50 vol.% H_2 and N_2 under pace velocity of 80, 000 ml h^{-1} g_{cat}^{-1}.

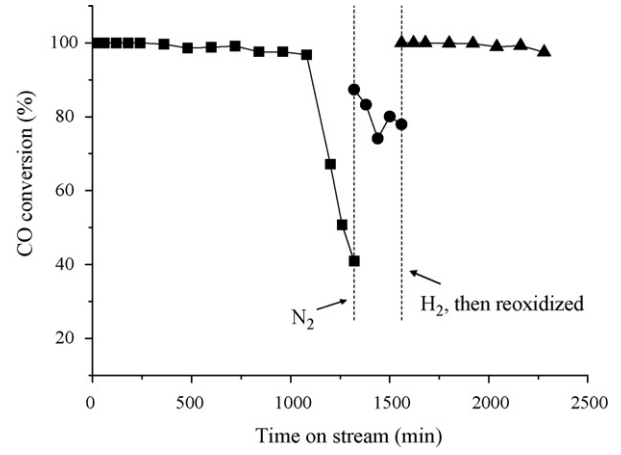

Fig. 4. Variation of CO conversion with reaction time over 8Co-1Ce-1Mn catalyst at 170 °C, under the space velocity of 80, 000 ml h^{-1} g_{cat}^{-1} and in reaction gas of 1 vol.% CO, 1 vol.% O_2, 50 vol.% H_2, 20 vol.% CO_2, 10 vol.% H_2O and N_2: (■) preliminary study; (●) after treated with N_2 at 300 °C for 30 min; (▲) treated with 5% H_2/N_2 at 250 °C for 30 min, and then treated with N_2 and 5%O_2/N_2 at 300 °C for 30 min respectively to reoxidize the reduced catalyst.

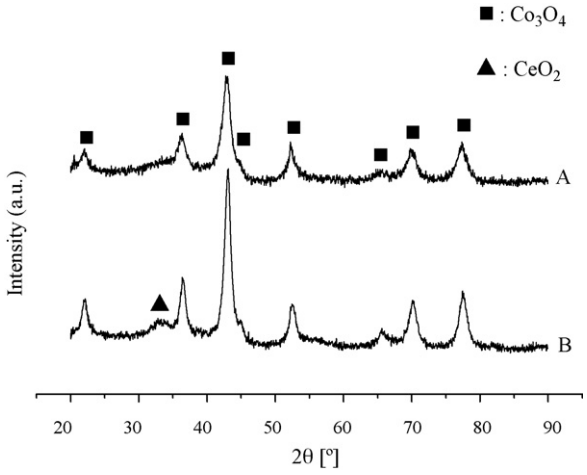

Fig. 5. XRD patterns of (A) 8Co-1Ce-1Mn and (B) 8Co-1Ce catalysts.

Fig. 6$B_{outside}$ and B_{inside}. In the area outside the circle of Fig. 6B, CeO_2 particles could hardly be seen by TEM, neither could cerium be detected by EDX technique. On the contrary, cerium could be detected inside the circle of Fig. 6B. These results showed that CeO_2 and Co_3O_4 particles were not uniformly mixed and ceria particles preferably congregated themselves in Co_3O_4–CeO_2 catalysts.

The TEM micrographs of 8Co-1Ce-1Mn catalyst are shown in Fig. 7A and B. It could be noted that Co_3O_4 particles became smaller, in agreement with the XRD results, and ceria dispersed much more uniformly when adding MnO_x into the 8Co-1Ce sample. At high magnification (Fig. 7B), CeO_2 particles which were shown in the black circles could be distinguished by the space distance between crystal face of 0.314 nm typical of crystalline ceria. As could be seen from the circles of Fig. 7B, ceria dispersed uniformly and were in contact with Co_3O_4 particles compactly. Manganese oxides particles could not be seen in the TEM images but could be detected by the EDX analysis. This indicated that MnO_x exhibited as much small particles or amorphous species, being consistent with XRD results. The copper in the EDX came from sample holding mesh which is made of copper.

The TPR results of Co_3O_4, 8Co-1Ce, 8Co-1Mn and 8Co-1Ce-1Mn catalysts are shown in Fig. 8 and Table 1. Pure cobalt oxides exhibited two reduction peaks signed as α and β corresponding to the reduction of Co_3O_4 to CoO and CoO to Co^0, respectively. This was in accordance with literature [31]. And the ratio of the peak area of α to β was about 1:3.2 which was close to 1:3, the ratio of two-step theoretical reduction of Co_3O_4.

Previous TPR studies had shown that the reduction behavior of Co_3O_4 could be strongly affected by supports [32]. In present case, adding ceria led to a new reduction peak signed as γ in Fig. 8. The γ peak should be attributed to the reduction of Co^{2+} interacting with ceria, which was in agreement with Spadaro [33] who proposed that Co_3O_4 in Co_3O_4/CeO_2 catalysts could be reduced as following steps:

(1) Reduction of the Co_3O_4 amorphous or crystalline phase to CoO.

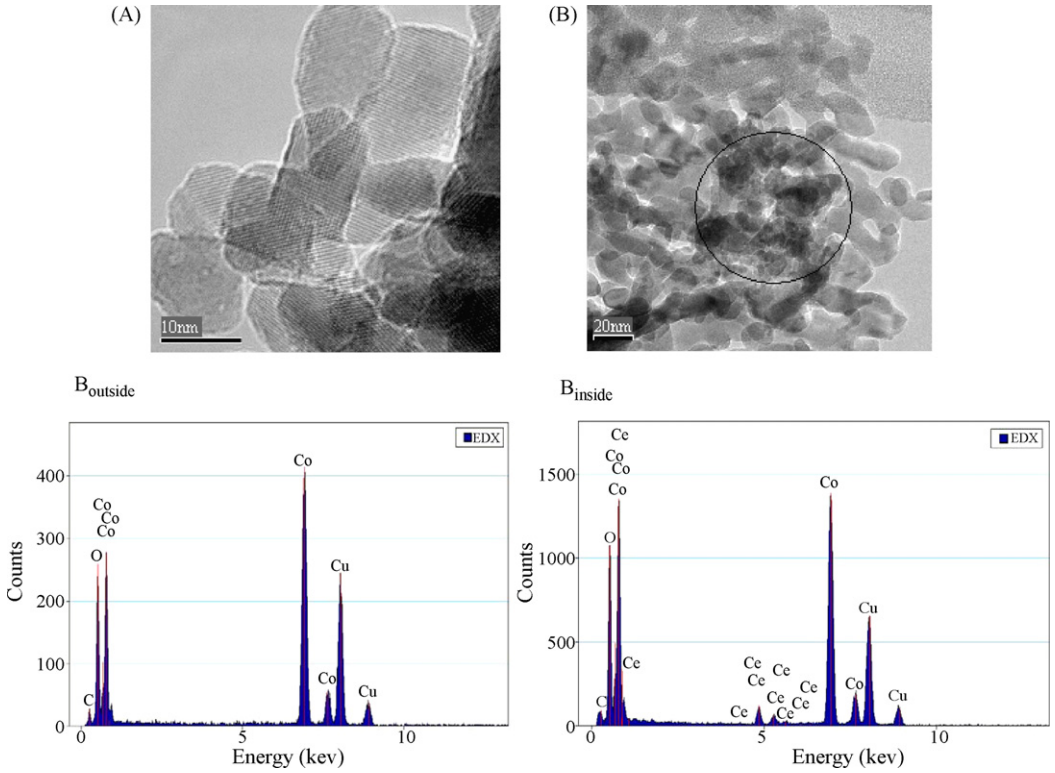

Fig. 6. TEM micrographs (A and B) and the EDX ($B_{outside}$ and B_{inside}) spectra of 8Co-1Ce catalyst. ($B_{outside}$) is the EDX analysis result of the area outside the circle of micrograph (B), and (B_{inside}) is the EDX analysis result of the area inside the circle of micrograph (B).

(2) Reduction of CoO particles coming from Co_3O_4 reduction and/or presenting in an amorphous/crystalline phase to Co^0.
(3) Reduction of small CoO clusters and/or Co^{2+} ions interacting with CeO_2.

The γ peak might contain the reduction peak of Ce^{4+} to Ce^{3+}. But the corresponding H_2 consumption for the ceria reduction should be much smaller than that for Co^{2+} reduction, because of the low content of CeO_2 in 8Co-1Ce catalyst and the partial reduction of Ce^{4+} to Ce^{3+} [34].

In Fig. 8, the TPR profiles of Co_3O_4 and 8Co-1Mn were similar, suggesting that the addition of a small amount of MnO_x had little influence on the reduction behavior of Co_3O_4. It was reported that Mn^{n+} could easily be reduced to MnO between 200 and 500 °C [35,36]. Due to the low content of manganese, the reduction peaks of Mn^{n+} were much smaller than that of cobalt ions. And the reduction peaks related to Mn^{n+} reduction should overlap with the reduction peaks of Co_3O_4.

The β peak disappeared and the area of γ peak became larger when adding a small mount of MnO_x into 8Co-1Ce catalyst. This should be due to the enhancement of the dispersion of ceria which resulted in the improvement of the interaction between Co^{n+} ions and CeO_2. As stated above, TEM and EDX results showed that the uniformity of the mixing of ceria and Co_3O_4 was largely improved by adding MnO_x. The congregated cobalt oxides particles, as a result, were replaced by dispersed Co_3O_4 particles which were in contact with CeO_2 compactly. Therefore, the β peak resulted from reduction of congregated CoO particles which had no contact with ceria disappeared, and the area of γ peak owing to the reduction of Co^{2+} interacting with CeO_2 increased.

It was proposed that higher valence state of cobalt, i.e. higher Co^{3+}/Co^{2+} ratio in CoO_x, would lead to higher catalytic activity for CO oxidation [24]. By neglecting the hydrogen consumption corresponding to ceria reduction and deducting the hydrogen consumption attributed to Mn^{n+} reduction, the ratios of Co^{3+}: Co^{2+} in these samples can be calculated from the hydrogen consumption (listed in Table 1). The calculated results of Co^{3+}:Co^{2+} ratios in Co_3O_4, 8Co-1Ce and 8Co-1Ce-1Mn samples were 1:0.6, 1:0.4 and 1:0.2–0.3 (for the valence state of Mn^{n+} was between +3 and +4), respectively. Therefore, adding ceria to pure cobalt oxides led to the Co^{3+}/Co^{2+} ratio increase, consistent with the proposal of Kang et al. [24] and adding MnO_x into 8Co-1Ce sample could further enhance the Co^{3+}/Co^{2+} ratio.

Fig. 9 shows the Co $2p_{3/2}$ XP spectra of Co_3O_4, 8Co-1Ce and 8Co-1Ce-1Mn samples and the deconvolution of Co $2p_{3/2}$ XP spectra by the program of XPS Peak4.1. Table 2 lists the binding energies and satellite ratios of the samples. Co_3O_4 contains two distinct types of cobalt ion, Co^{2+} in tetrahedral sites and Co^{3+} in octahedral sites [37]. The $2p_{3/2}$ binding energy of Co^{2+} is close to that of Co^{3+}, while the two oxidation states of cobalt can be distinguished by a distinct shake up satellite of Co^{2+} [38]. With adding ceria into pure Co_3O_4, the satellite ratio decreased from 0.41 to 0.32, meaning the ratio of Co^{3+}/Co^{2+} became higher, which was in agreement with TPR results and reference [24]. The satellite ratio in 8Co-1Ce-1Mn catalyst was lower than that in 8Co-1Ce catalyst, indicating that MnO_x

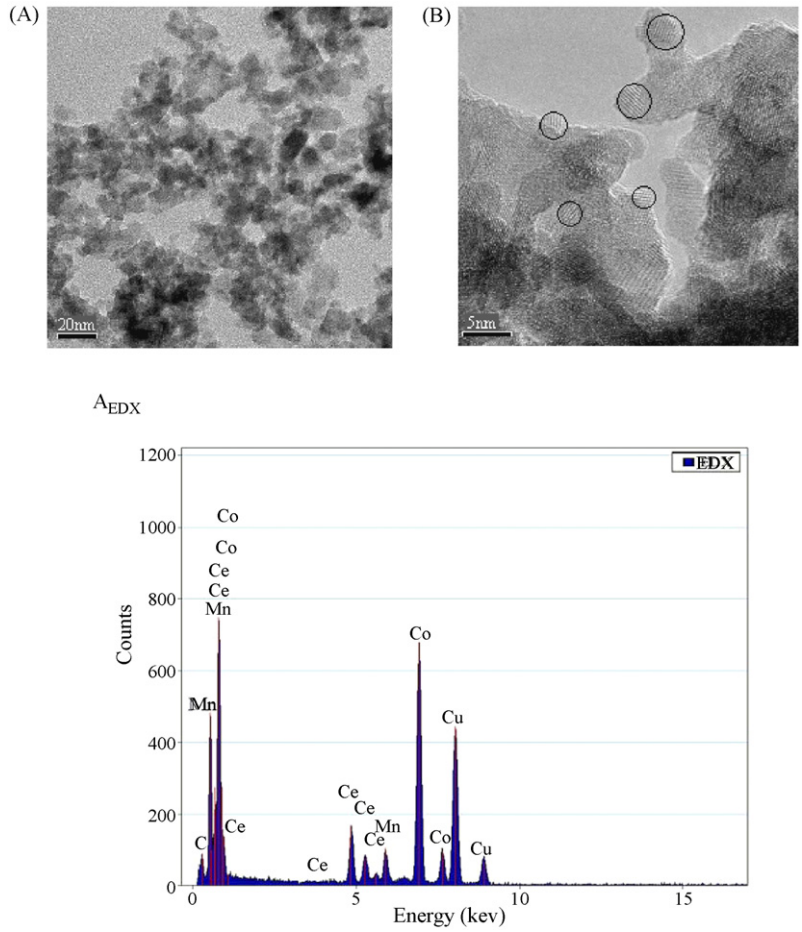

Fig. 7. TEM micrographs of 8Co-1Ce-1Mn catalyst (A and B) and corresponding EDX results (A_{EDX}).

further enhanced the valence state of Co_3O_4, in accordance with TPR results.

Our previous work [29] showed that the catalytic performance of Co_3O_4 for CO-PROX was markedly improved by adding ceria. Kang et al. studied the activity of CoO_x/CeO_2 catalysts for CO oxidation and proposed that the high activity of CoO_x/CeO_2 for CO oxidation was ascribed to the finely dispersed and high valence state CoO_x species, and pointed out that ceria provided oxygen to cobalt which retained higher valence state of cobalt [24]. TEM, EDX and TPR results in this work showed that ceria and Co_3O_4 in 8Co-1Ce catalyst did not mixed uniformly and there were still a large mount of congregated Co_3O_4 particles which were not in contact with CeO_2. Those Co_3O_4 particles which were not in contact with ceria had no interaction with CeO_2 accordingly, and thus should be less active. On the other hand, for MnO_x modified Co_3O_4-CeO_2 catalysts, XRD, TEM and TPR results showed that Co_3O_4 and CeO_2 particles were well mixed and in compact contact with each other which led to cobalt oxides in higher dispersion and higher valence state. The catalytic performance of 8Co-1Ce

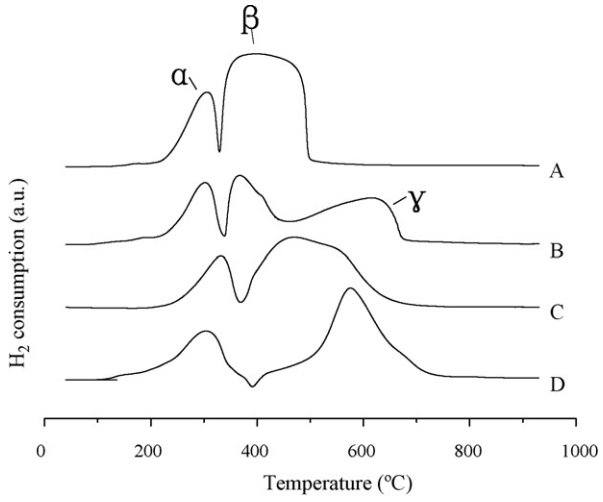

Fig. 8. TPR profiles of (A) Co_3O_4, (B) 8Co-1Ce, (C) 8Co-1Mn and (D) 8Co-1Ce-1Mn catalysts.

Table 1
The amounts of consumed hydrogen during TPR experiments and Co^{3+}/Co^{2+} ratios calculated from hydrogen consumption

Samples	H_2 consumption ($\mu mol/g_{cat}$)		The ratios of Co^{3+}:Co^{2+}
	α peak	β and γ peaks	
Co_3O_4	3750	12,037	1:0.6
8Co-1Ce	3174	8,728	1:0.4
8Co-1Mn	2686	9,895	–
8Co-1Ce-1Mn	3983	8,539	1:0.2–0.3

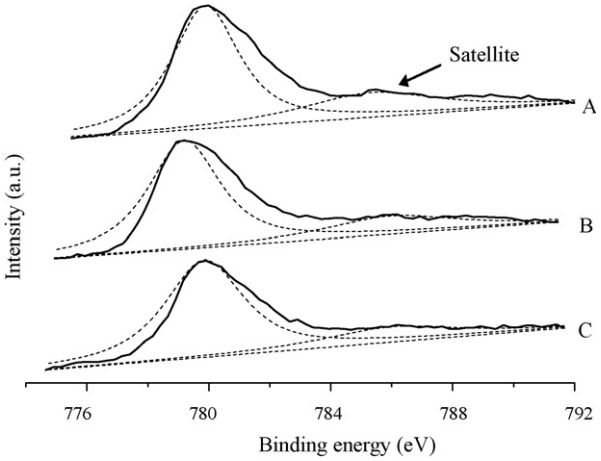

Fig. 9. Co $2p_{3/2}$ XP spectra of (A) Co_3O_4, (B) 8Co-1Ce and (C) 8Co-1Ce-1Mn catalysts. Solid line: Original Co $2p_{3/2}$ XP spectra; Dash line: Deconvolution of Co $2p_{3/2}$ XP spectra.

catalysts for CO-PROX, therefore, was significantly improved by adding a small mount of MnO_x. These results support the viewpoint proposed by Kang et al. [24] that high activity of Co_3O_4-CeO_2 for CO oxidation is ascribed to the finely dispersed and high valence state Co_3O_4.

The activity for H_2 oxidation did not increase so largely as the improvement for CO oxidation by adding MnO_x into 8Co-1Ce catalyst, which resulted in the high selectivity to CO oxidation. Generally, the activation energy for the oxidation of carbon monoxide is lower than that for the oxidation of hydrogen. So H_2 can hardly be oxidized as CO conversion is at a relatively low level at a relatively low reaction temperature accordingly. With increasing temperature, hydrogen gets enough energy to overcome the activation barrier to compete with CO for adsorption and oxidation on the surface of catalysts, which leads to the decrease of selectivity to CO oxidation. For the reported CO-PROX catalysts so far, if CO can be oxidized at low temperature, the temperature for H_2 oxidation over the same catalyst is relatively low as well; on the other side, if a catalyst is active at relatively higher temperature for CO oxidation, the temperature for H_2 oxidation increases correspondingly. Thus, the temperature windows for complete CO removal over different catalysts are similar, about 20 °C [2,9,18,39]. However, 8Co-1Ce-1Mn catalyst in this work showed much broader temperature window for 100% CO conversion. The reason for this high selectivity to CO oxidation need to be further investigated.

Table 2
XPS results

Catalysts	Co $2p_{3/2}$ (eV)	Shake-up Co $2p_{3/2}$ (eV)	Satellite ratio
CoO[a]	781.0	786.8	–
Co_3O_4[a]	780.3	–	–
Co_3O_4[b]	780.1	784.4	0.41
8Co-1Ce[b]	779.9	786.7	0.32
8Co-1Ce-1Mn[b]	779.8	786.1	0.26

[a] Cited from Ref. [38].
[b] This work.

4. Conclusion

The catalytic performance of Co_3O_4-CeO_2 catalysts for CO preferential oxidation in H_2-rich gases can be effectively improved by MnO_x modification. Co-Ce-Mn mixed oxides catalyst with proper Co:Ce:Mn ratio is a promising candidate for CO removal from hydrogen-rich gases.

The addition of MnO_x into Co_3O_4-CeO_2 catalysts leads to uniform mixing of cobalt oxide and nano-ceria particles which is beneficial for the formation of interaction between cobalt oxides and ceria. The interaction between Co_3O_4 and CeO_2 results in finely dispersed and high valence state cobalt oxides species which contribute to the high catalytic activity of Co-Ce-Mn mixed oxides catalyst for CO-PROX.

Acknowledgments

The financial support of this work by Hi-tech Research and Development Program of China (863 program, Granted as No. 2006AA05Z115), National Natural Science Foundation of China (No. 20476079) and the Cheung Kong Scholar Program for Innovative Teams of the Ministry of Education (No. IRT0641) are gratefully acknowledged.

References

[1] C. Song, Catal. Today 77 (2002) 17–49.
[2] G. Avgouropoulos, T. Ioannides, Ch. Papadopoulou, J. Batista, S. Hocevar, H.K. Matralis, Catal. Today 75 (2002) 157–167.
[3] M. Watanabe, H. Uchida, K. Ohkubo, H. Igarashi, Appl. Catal. B 46 (2003) 595–600.
[4] G. Avgouropoulos, T. Ioannides, Appl. Catal. A 244 (2003) 155–167.
[5] C. Pedrero, T. Waku, E. Iglesia, J. Catal. 233 (2005) 242–255.
[6] A. Manasilp, E. Gulari, Appl. Catal. B 37 (2002) 17–25.
[7] Y. Minemura, M. Kuriyama, S. Ito, K. Tomishige, K. Kunimori, Catal. Commun. 7 (2006) 623–626.
[8] I.H. Son, M. Shamsuzzoha, A.M. Lane, J. Catal. 210 (2002) 460–465.
[9] P.V. Snytnikov, V.A. Sobyanin, V.D. Belyaev, P.G. Tsyrulnikov, N.B. Shitova, D.A. Shlyapin, Appl. Catal. A 239 (2003) 149–156.
[10] J.L. Ayastuy, M.P. Gonzalez-Marcos, J.R. Gonzalez-Velasco, M.A. Gutierrez-Ortiz, Appl. Catal. B 70 (2007) 532–541.
[11] Y.F. Han, M.J. Kahlich, M. Kinne, R.J. Behm, Appl. Catal. B 50 (2004) 209–218.
[12] B. Schumacher, Y. Denkwitz, V. Plzak, M. Kinne, R.J. Behm, J. Catal. 224 (2004) 449–462.
[13] L.H. Chang, N. Sasirekha, Y.W. Chen, W.J. Wang, Ind. Eng. Chem. Res. 45 (2006) 4927–4935.
[14] F. Arena, P. Famulari, G. Trunfio, G. Bonura, F. Frusteri, L. Spadaro, Appl. Catal. B 66 (2006) 81–91.
[15] G. Panzera, V. Modafferi, S. Candamanoa, A. Donato, F. Frusteri, P.L. Antonucci, J. Power Sources 135 (2004) 177–183.
[16] M.M. Schubert, A. Venugopal, M.J. Kahlich, V. Plzak, R.J. Behm, J. Catal. 222 (2004) 32–40.
[17] R.J.H. Grisel, C.J. Weststrate, A. Goossens, M.W.J. Crajé, A.M. vander Kraan, B.E. Nieuwenhuys, Catal. Today 72 (2002) 123–132.
[18] Y. Liu, Q. Fu, M.F. Stephanopoulos, Catal. Today 93–95 (2004) 241–246.
[19] G. Avgouropoulos, T. Ioannides, Appl. Catal. B 67 (2006) 1–11.
[20] J. Papavasiliou, G. Avgouropoulos, T. Ioannides, Appl. Catal. B 66 (2006) 168–174.

[21] E. Moretti, M. Lenarda, L. Storaro, A. Talon, R. Frattini, S. Polizzi, E. Rodriguez-Castellon, A. Jimenez-Lopez, Appl. Catal. B 72 (2007) 149–156.
[22] A. Martinez-Arias, A.B. Hungria, G. Munuera, D. Gamarra, Appl. Catal. B 65 (2006) 207–216.
[23] M.M. Schubert, M.J. Kahlich, H.A. Gasteiger, R.J. Behm, J. Power Sources 84 (1999) 175–182.
[24] M. Kang, M.W. Song, C.H. Lee, Appl. Catal. A 251 (2003) 143–156.
[25] M. Kang, M.W. Song, K.L. Kim, React. Kinet. Catal. Lett. 79 (2003) 3–10.
[26] Y. Teng, H. Sakurai, A. Ueda, T. Kobayashi, Int. J. Hydrogen Energy 24 (1999) 355–358.
[27] W.S. Epling, P.K. Cheekatamarla, A.M. Lane, Chem. Eng. J. 93 (2003) 61–68.
[28] K. Omata, Y. Kobayashi, M. Yamada, Catal. Commun. 8 (2007) 1–5.
[29] Q. Guo, Y. Liu, React. Kinet. Catal. Lett. 92 (2007) 19–25.
[30] F. Grillo, M.M. Natile, A. Glisenti, Appl. Catal. B 48 (2004) 267–274.
[31] L. Xue, C. Zhang, H. He, Y. Teraoka, Appl. Catal. B 75 (2007) 167–174.
[32] G.H. Philip, I.K. Ball, D. Wayne, L. Povilas, C. Matias, E.M. Eduardo, A.U. Maria, Chem. Eng. J. 95 (2003) 47–55.
[33] L. Spadaro, F. Arena, M.L. Granados, M. Ojeda, J.L.G. Fierro, F. Frusteri, J. Catal. 234 (2005) 451–462.
[34] W.J. Shan, M. Fleys, F. Lapicque, D. Swierczynski, A. Kiennemann, Y. Simon, P. Marquaire, Appl. Catal. A 311 (2006) 24–33.
[35] J. Villaseñor, P. Reyes, G. Pecchi, Catal. Today 76 (2002) 121–131.
[36] G. Picasso, M. Gutierrez, M.P. Pina, J. Herguido, Chem. Eng. J. 126 (2007) 119–130.
[37] T.J. Chuang, C.R. Brundle, D.W. Rice, Surf. Sci. 59 (1976) 413–429.
[38] N.N. Natile, A. Glisenti, Chem. Mater. 14 (2002) 3090–3099.
[39] A. Wootsch, C. Descorme, D. Duprez, J. Catal. 225 (2004) 259–266.